



Article

Phenolic Compounds Cannabidiol, Curcumin and Quercetin Cause Mitochondrial Dysfunction and Suppress Acute Lymphoblastic Leukemia Cells

Miguel Olivas-Aguirre , Liliana Torres-López , Igor Pottosin * and Oxana Dobrovinskaya *

Laboratory of Immunobiology and Ionic Transport Regulation, Centro Universitario de Investigaciones Biomédicas, Universidad de Colima, Av. 25 de Julio 965, Villa de San Sebastián, 28045 Colima, Mexico; miguel.a.olivas@gmail.com (M.O.-A.); lilianatorres4667@gmail.com (L.T.-L.)

* Correspondence: pottosin@ucol.mx (I.P.); oxana@ucol.mx (O.D.)

Abstract: Anticancer activity of different phenols is documented, but underlying mechanisms remain elusive. Recently, we have shown that cannabidiol kills the cells of acute lymphoblastic leukemia (ALL) by a direct interaction with mitochondria, with their consequent dysfunction. In the present study, cytotoxic effects of several phenolic compounds against human the T-ALL cell line Jurkat were tested by means of resazurin-based metabolic assay. To unravel underlying mechanisms, mitochondrial membrane potential ($\Delta\Psi_m$) and $[Ca^{2+}]_m$ measurements were undertaken, and reactive oxygen species generation and cell death were evaluated by flow cytometry. Three out of eight tested phenolics, cannabidiol, curcumin and quercetin, which displayed a significant cytotoxic effect, also dissipated the $\Delta\Psi_m$ and induced a significant $[Ca^{2+}]_m$ increase, whereas inefficient phenols did not. Dissipation of the $\Delta\Psi_m$ by cannabidiol was prevented by cyclosporine A and reverted by Ru360, inhibitors of the permeation transition pore and mitochondrial Ca^{2+} uniporter, respectively. Ru360 prevented the phenol-induced $[Ca^{2+}]_m$ rise, but neither cyclosporine A nor Ru360 affected the curcumin- and quercetin-induced $\Delta\Psi_m$ depolarization. Ru360 impeded the curcumin- and cannabidiol-induced cell death. Thus, all three phenols exert their antileukemic activity via mitochondrial Ca^{2+} overload, whereas curcumin and quercetin suppress the metabolism of leukemic cells by direct mitochondrial uncoupling.

Keywords: acute lymphoblastic leukemia; cannabidiol; curcumin; quercetin; mitochondria; cytotoxicity



Citation: Olivas-Aguirre, M.; Torres-López, L.; Pottosin, I.; Dobrovinskaya, O. Phenolic Compounds Cannabidiol, Curcumin and Quercetin Cause Mitochondrial Dysfunction and Suppress Acute Lymphoblastic Leukemia Cells. *Int. J. Mol. Sci.* **2021**, *22*, 204. <https://dx.doi.org/10.3390/ijms22010204>

Received: 29 November 2020

Accepted: 23 December 2020

Published: 28 December 2020

Publisher's Note: MDPI stays neutral with regard to jurisdictional claims in published maps and institutional affiliations.



Copyright: © 2020 by the authors. Licensee MDPI, Basel, Switzerland. This article is an open access article distributed under the terms and conditions of the Creative Commons Attribution (CC BY) license (<https://creativecommons.org/licenses/by/4.0/>).

1. Introduction

Cancer represents a main cause of morbidity and mortality worldwide. Acute lymphoblastic leukemia (ALL) is an aggressive hematologic disorder that occurs mainly in children and adolescents. T-lineage ALL (T-ALL) represents a clinical challenge due its multiple mechanisms of chemotherapy resistance and cell death evasion, responsible for patient chemotherapy failure, relapse and death [1,2]. Therefore, the search for novel antileukemic compounds with a high anticancer effectiveness and low side effects continues.

Phenolic compounds are a group of phytochemicals, containing one or several aromatic rings, which are commonly obtained from plants, vegetables and common beverages such as beer, red wine or coffee. They received attention primarily due to their antioxidant activity. Yet, phenolic compounds possess a broader spectrum of action, including cytotoxic effects in different cancer types [3–5]. Previous studies have suggested that high consumption of phenols may reduce cancer risks. Related mechanisms include, but are not restricted to, modifications in the antioxidant system, receptor-mediated cell signaling, cell cycle modifications and cell death induction. Importantly, the anticancer effect of phenols seems to be highly dependent on phenol species and cancer type [6].

Antileukemic activity was demonstrated for several phenolic compounds, albeit precise step-by-step mechanisms remain elusive. Reported effects include a decrease in cancer cells population in vitro and in vivo, deregulation of the Bcl-2 protein ratio, caspase activation, reactive oxygen species (ROS) production, cytochrome c release and apoptosis induction (Table S1).

Recently, targeting to mitochondria, which provokes their dysfunction, was demonstrated for several small molecules containing phenolic groups, such as ellagic acid, curcumin, aspirin and cannabidiol (CBD) [7–10]. Several phenols with a pKa within the physiological range possess protonophore activity, thus efficiently dissipating the electrochemical gradient for H⁺ across the inner mitochondrial membrane and, in this way, suppressing different cancer cell types [11]. Notably, leukemic mitochondria have been proposed as an attractive target for anticancer therapy. Mitochondria acquire different alterations during malignant reprogramming that make them susceptible to small molecules with anticancer activity, known as mitocans, which include phenolic compounds [12,13].

We have recently demonstrated that CBD, a main phytocannabinoid derived from *Cannabis* spp., kills leukemic cells by directly targeting mitochondria and causing ROS generation, mitochondrial calcium ([Ca²⁺]_m) overload, stable mitochondrial permeability transition pore (mPTP) formation and cytochrome c release, which eventually promotes apoptosis and mPTP-driven necrosis [10]. Western blot data and experiments with isolated voltage-dependent anion channel (VDAC) protein, incorporated into a planar lipid bilayer, demonstrated that CBD directly interacts with and switches VDAC to a closed conformational substate [14]. A similar mechanism was also reported for curcumin and aspirin and is considered to be the cause of the tumor cell death [8,9]. VDAC is unique porin, functionally present and abundant in the outer mitochondrial membrane. It acts as the mitochondrial gatekeeper, mediating ionic and metabolic fluxes between the cytosol and the mitochondrial intermembrane space [15–17]. The selectivity of this exchange critically depends on the conformational state of VDAC. The aforementioned closed conformational substate is impermeable for large metabolites like adenine nucleotides, but highly permeable to Ca²⁺ [15]. The combination of these two factors can eventually lead to mitochondrial Ca²⁺ overload [10].

The purpose of the present work was to test the cytotoxic effects of several phenolic compounds with a documented antileukemic activity, using the human Jurkat cell line as a model for acute lymphoblastic leukemia of T type (T-ALL). Specifically, we wish to unravel whether the anti-T-ALL activity of the phenolics is correlated with their effects on ROS generation and alterations of the mitochondrial parameters, such as electrical potential difference and Ca²⁺ homeostasis, and whether the prevention of the latter can revert the cytotoxicity.

2. Results

2.1. Comparison of Antileukemic Properties of Different Phenolic Compounds in T-ALL Model

Eight phenol-containing compounds that were reported earlier to possess cytotoxic properties against different types of leukemia (Table S1) were selected to compare their antileukemic potential against T-ALL-derived Jurkat cells. A metabolic activity assay showed that CBD and curcumin were the most cytotoxic, with an IC₅₀ of 12.1 and 36.5 μM, respectively (Figure 1). Chlorogenic and gallic acid, as well as quercetin, exhibited a mild cytotoxicity, whereas aspirin, methyl gallate and protocatechuic acid at concentrations up to 2.5 mM lacked any substantial effect at 24 h.

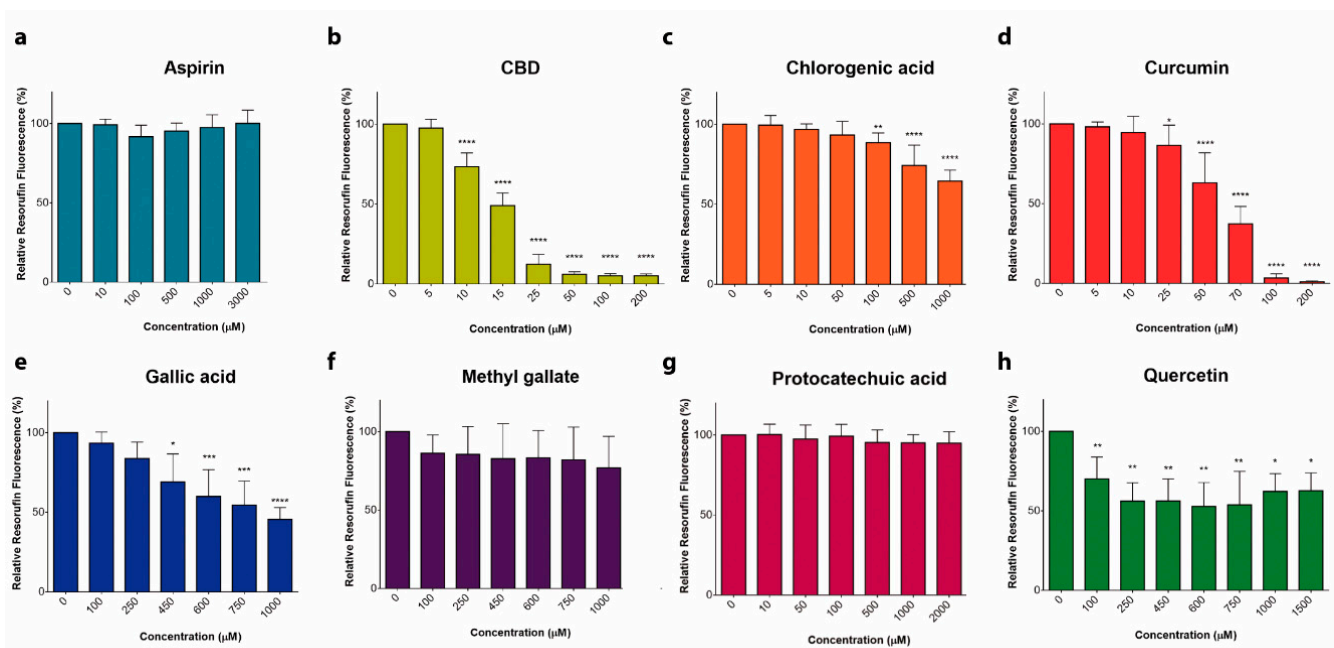


Figure 1. Cytotoxic effect of phenols on leukemic cells. (a–f) Cytotoxic effect of phenolic compounds was estimated by means of resazurin-based metabolic assay. T-ALL cells (Jurkat) were incubated in the presence or absence of aspirin (a), cannabidiol, CBD (b), chlorogenic acid (c), curcumin (d), gallic acid (e), methyl gallate (f), protocatechuic acid (g) and quercetin (h), for 24 h. Resorufin fluorescence was measured and normalized to untreated cells. Data are mean \pm SD ($n = 9$ from three independent experiments; * $p < 0.05$; ** $p < 0.01$; *** $p < 0.001$; **** $p < 0.0001$; one-way ANOVA). Non-linear fit of the dose-dependence yields the following IC50 values (in μM): 12.1 for CBD and 36.5 for curcumin.

2.2. Curcumin is Rapidly Taken Up by Mitochondria

Some phenolic compounds cause cell death by targeting mitochondria [4,10,17]. We took the advantage of the intrinsic fluorescence of curcumin (Figure 2a) to monitor its uptake and subsequent subcellular localization [18]. Jurkat cells incorporated curcumin rapidly after 10 min of treatment (Figure 2b). Confocal microscopy assays revealed that curcumin was selectively localized in discrete puncta in cytosol (Figure 2c). To determine whether these regions correspond to mitochondria, cells were stained with the mitochondrial-selective dye Mitotracker Red (MtRed) prior to the curcumin treatment. High co-localization of MtRed and curcumin fluorescence (Figure 2d–e) indicates that mitochondria are primary targets for curcumin. Thus, the effect of phenolic compounds on the transmembrane electrical potential difference, whose magnitude reflects the mitochondrial energized status, was further addressed.

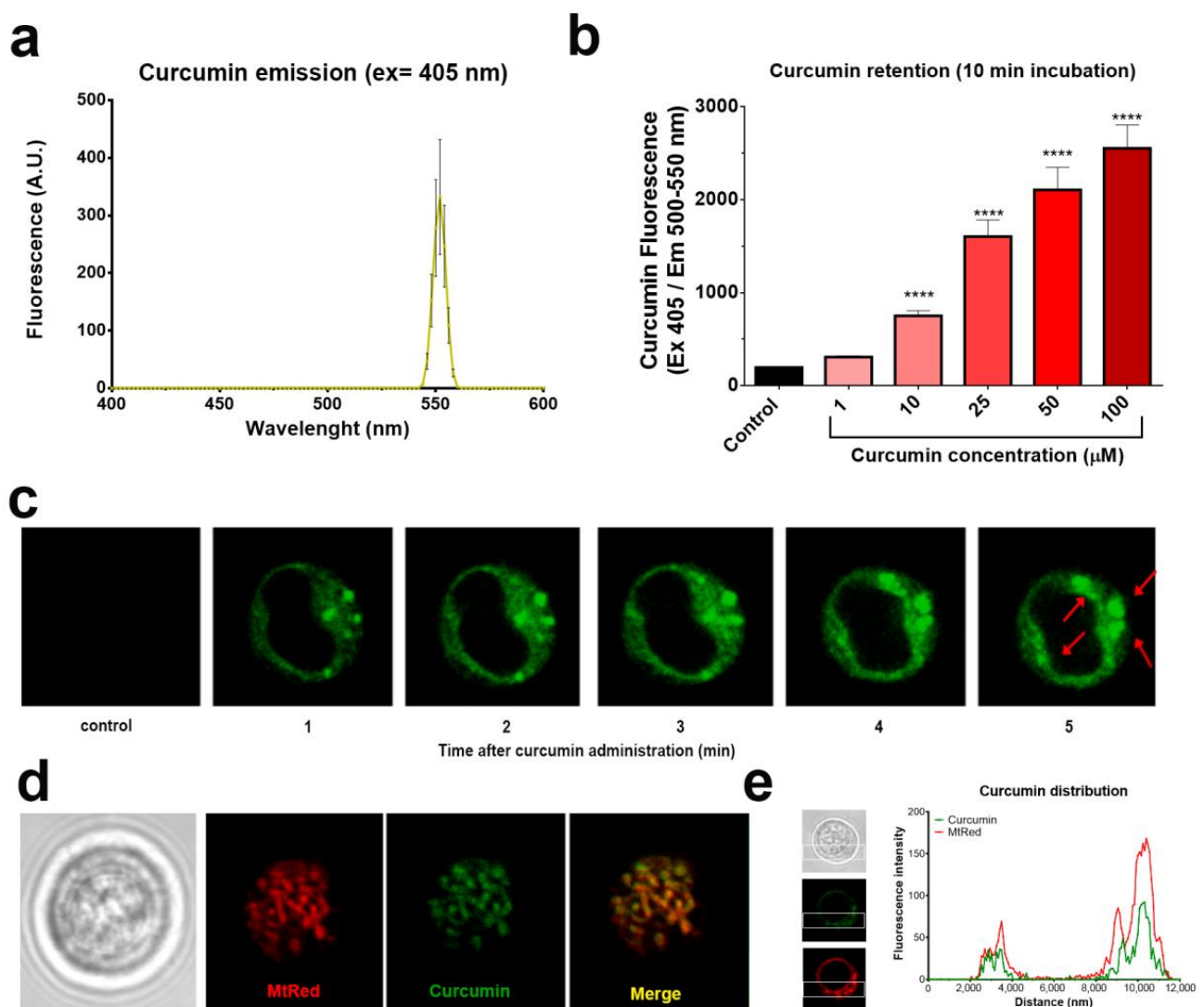


Figure 2. Curcumin is rapidly taken up by mitochondria in T-ALL cells. (a) Curcumin ($50 \mu\text{M}$) autofluorescence estimated by spectrofluorometry. (b) Dose-dependent uptake of curcumin by Jurkat cells. Data are mean \pm SD ($n = 12$ from three independent experiments; **** $p < 0.0001$; one-way ANOVA). (c) Time course of curcumin ($25 \mu\text{M}$) uptake (green) by Jurkat cells. Red arrows indicate puncta of curcumin accumulation. (d) Co-localization of curcumin ($25 \mu\text{M}$, 10 min incubation) with the mitochondrial-selective fluorophore Mitotracker Red (MtRed). (e) Spatial distribution of curcumin and MtRed fluorescence intensity along the cell axis within a single Jurkat cell.

2.3. Cytotoxic Phenols Promote Mitochondrial $[\text{Ca}^{2+}]_m$ Overload and $\Delta\Psi_m$ Loss

We previously found out that CBD evoked mitochondrial Ca^{2+} ($[\text{Ca}^{2+}]_m$) overload, resulting in a stable mitochondrial mPTP formation, $\Delta\Psi_m$ loss and cell death [10]. These phenomena have also been observed in cells of other types of cancers that were exposed to various phenols [9,19–21]. In addition to CBD, curcumin and quercetin, which also demonstrated the capacity to compromise Jurkat cell viability (Figure 1), promoted an immediate $[\text{Ca}^{2+}]_m$ overload (Figure 3a–b). Contrary to these three phenolic compounds, aspirin or chlorogenic acid, which did not exhibit a significant cytotoxicity, provoked an insignificant $[\text{Ca}^{2+}]_m$ rise (Figure 3a–b).

To compare the effect of different phenolic compounds on $\Delta\Psi_m$, tetramethylrhodamine ethyl ester perchlorate (TMRE) fluorescence was evaluated in TMRE-stained cells (Figure 3c). In line with their cytotoxic effects, CBD, curcumin and quercetin produced an immediate $\Delta\Psi_m$ collapse (cf. positive control with a classical uncoupler, CCCP). The depo-

larized state persisted after 4 and 8 h (Figure 3e,g,k), whereas chlorogenic acid and methyl gallate only slightly diminished $\Delta\Psi_m$ at 8 h (Figure 3f,i), and protocatechuic acid had no significant effect at 4–8 h (Figure 3j). Notably, aspirin and gallic acid favored the TMRE retention (Figure 3d,h), which implies a hyperpolarization instead of a depolarization.

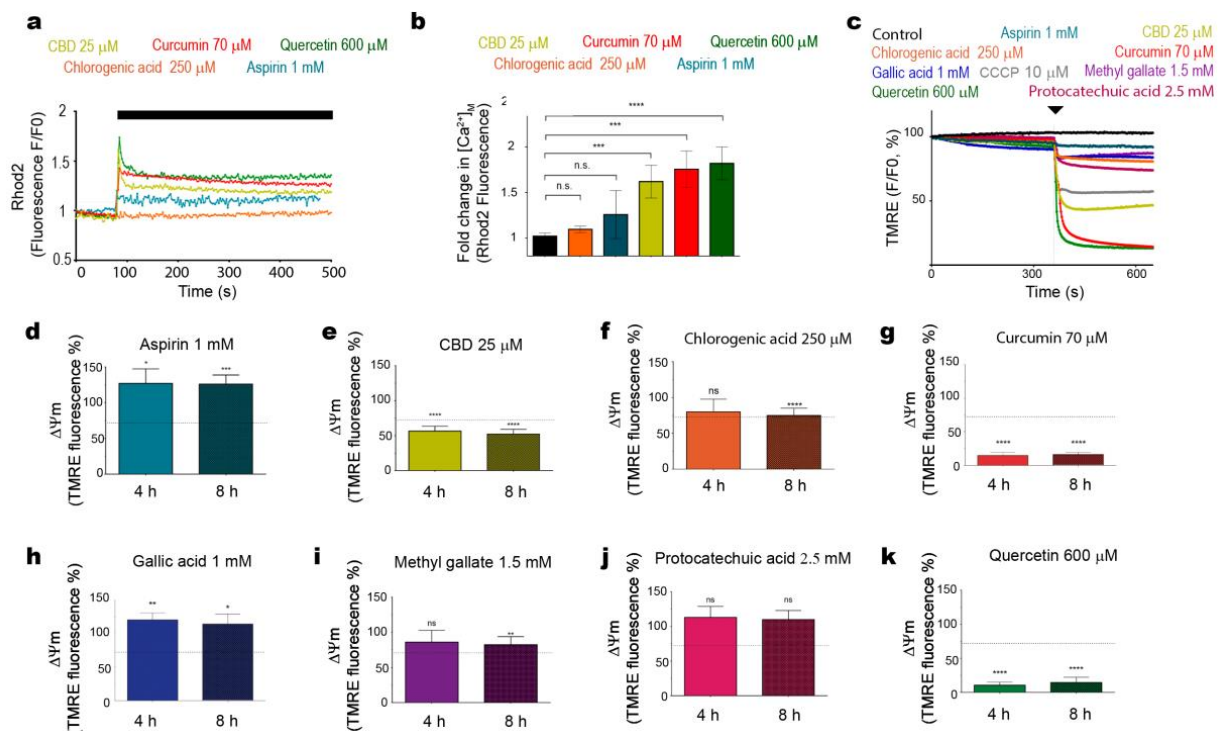


Figure 3. Effects of phenolic compounds on mitochondrial Ca^{2+} and $\Delta\Psi_m$. (a) Jurkat cells stained with mitochondrial Ca^{2+} indicator Rhod-2 AM (2 μ M) were treated with curcumin (red trace), CBD (yellow trace), aspirin (blue trace), chlorogenic acid (orange trace) or quercetin (green trace). The effect of phenols on Rhod-2 fluorescence was evaluated by spectrofluorometry and normalized to initial fluorescence of untreated cells. Traces represent the average of three samples from independent experiments \pm SD. (b) The amplitude of $[Ca^{2+}]_m$ response (peak- $[Ca^{2+}]_m$ level prior drug administration) was averaged and plotted as mean \pm SD for each phenol and compared to unstimulated cells ($n = 6$ from three independent experiments; ns: not significant; **** $p < 0.0001$; one-way ANOVA). The immediate effect of phenols on $\Delta\Psi_m$ in tetramethylrhodamine ethyl ester perchlorate (TMRE)-stained Jurkat cells was evaluated by spectrofluorometry (c). Traces represent the average of three samples from independent experiments. (d–k) The effect of aspirin (d), CBD (e), chlorogenic acid (f), curcumin (g), gallic acid (h), methyl gallate (i), protocatechuic acid (j) or quercetin (k) on $\Delta\Psi_m$ in TMRE-stained Jurkat cells at 4 and 8 h of treatment. Data are compared with a positive control (CCCP, 10 μ M, 4 h, dashed line). TMRE fluorescence intensity in untreated cells is taken as 100%, data are mean \pm SD ($n = 9$ from three independent experiments; ns: not significant; * $p < 0.05$; ** $p < 0.01$; *** $p < 0.001$; **** $p < 0.0001$; one-way ANOVA).

2.4. Mitochondrial Uncoupling and Ca^{2+} Overload Mediate the Cytotoxic Effect of Bioactive Phenols

$\Delta\Psi_m$ loss can be attributed to the mPTP formation or the protonophore activity of phenols. To determine the dependence of mPTP-mediated $\Delta\Psi_m$ loss, Jurkat cells were stained with TMRE and preincubated with the mPTP inhibitor CsA (10 μ M, 20 min preincubation). Under this condition, mPTP inhibition suppressed the CBD effects on $\Delta\Psi_m$. However, the depolarization induced by curcumin and quercetin was unaffected in the presence of CsA (Figure 4a). Inhibition of $[Ca^{2+}]_m$ overload by mitochondrial Ca^{2+} uniporter, MCU, blocker Ru360 (1 μ M, 20 min preincubation) reverted the $\Delta\Psi_m$ loss induced by CBD but not that by curcumin or quercetin (Figure 4b,c). Thus, curcumin and quercetin may act as direct uncouplers, whereas $[Ca^{2+}]_m$ overload was necessary for the mPTP formation and $\Delta\Psi_m$ dissipation in CBD-treated cells. To evaluate the effect of $[Ca^{2+}]_m$ overload inhibition

on cell death induced by phenols, Jurkat cells were treated with CBD (25 μM), curcumin (200 μM) or quercetin (1.5 mM) for 1 h and stained with DAPI as a cell death marker. Cytotoxic effects were rapidly observed for CBD- and curcumin-treated cells (Figure 4d) and were to a great extent prevented by Ru360. Metabolic activity of Jurkat cells was decreased by all three phenols, but only in the case of CBD did Ru360 display a significant protection (Figure 4e), in agreement with previous results [10].

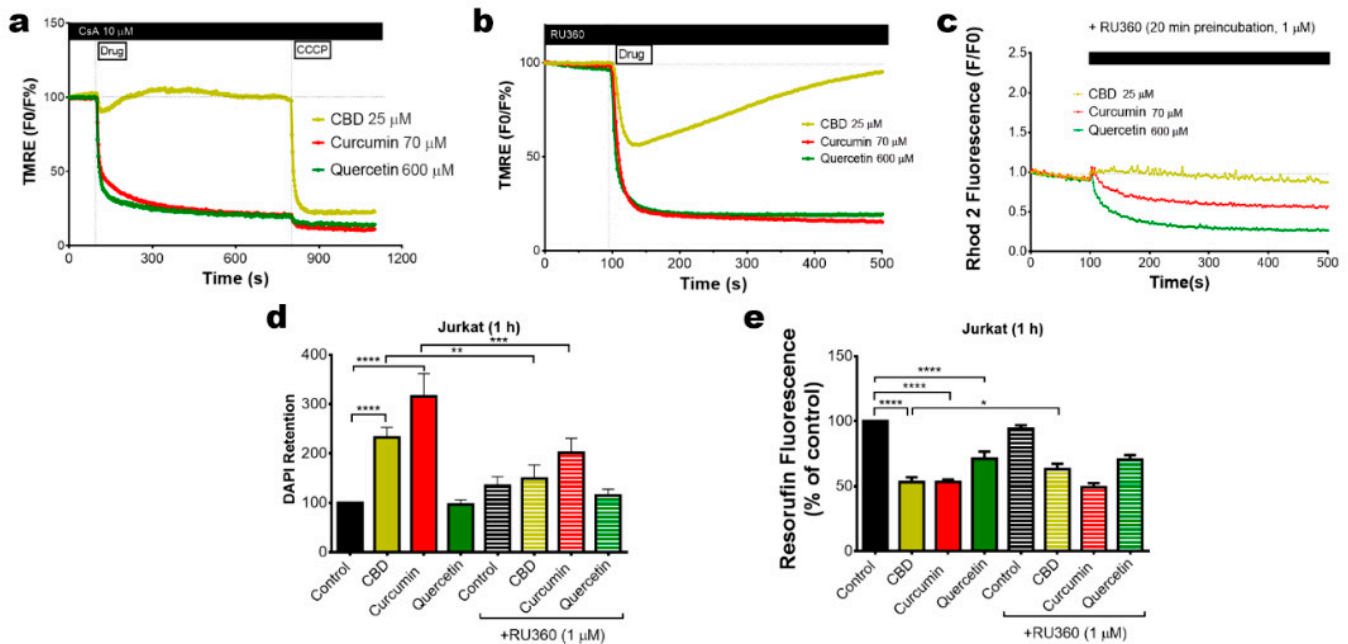


Figure 4. Pharmacology of the mitochondrial Ca^{2+} and $\Delta\Psi_m$ changes induced by cytotoxic phenols. (a) The effect of the mPTP inhibitor (CsA, 20 min preincubation) on $\Delta\Psi_m$ in TMRE-stained Jurkat cells, treated with phenols. Traces represent the average of three independent experiments. CCCP (10 μM) was added as a control at the end of each experiment. (b) Effect of Ru360 (1 μM , 20 min preincubation) on $\Delta\Psi_m$ in TMRE-stained Jurkat cells, treated with phenols. Traces represent the average of three independent experiments. (c) Effect of the MCU inhibitor Ru360 preincubation (1 μM) over the mitochondrial Ca^{2+} changes, induced by phenols, in Jurkat cells stained with Rhod-2 (2 μM). Traces represent the average of three independent experiments. Effect of Ru360 (1 μM , 20 min preincubation) on the cell death (d) or metabolism (e) of Jurkat cells, treated with CBD (25 μM), curcumin (70 μM) or quercetin (600 μM). Bars represent the average of three independent experiments \pm SD, analyzed by a one-way ANOVA test (* $p < 0.05$; ** $p < 0.01$; *** $p < 0.001$; **** $p < 0.0001$).

2.5. Phenols Differentially Regulate ROS Production

Alteration of the $\Delta\Psi_m$, by either depolarization, associated with the mPTP opening, or hyperpolarization, due to a hyperactive oxidative phosphorylation, both cause an increase in ROS generation by mitochondria, which can eventually lead to cell death [22–24]. On the other hand, phenols per se can act as ROS scavengers. To assess the functional impact of phenolic compounds on the net ROS production, cells were treated with phenols for 1 and 2 h and ROS production was evaluated by flow cytometry using 2', 7'-Dichlorodihydrofluorescein diacetate, DCFH-DA. Under our experimental conditions, aspirin, CBD and curcumin triggered an elevation in the ROS production as compared to untreated cells (Figure 5a–d). This ROS elevation was transient and undetectable at 2 h post-administration. Meanwhile, gallic acid, methyl gallate, protocatechuic acid and quercetin tend to decrease basal ROS levels, thereby demonstrating antioxidant properties (Figure 5e–h). Apparently, pro- or antioxidant activity of phenolic compounds per se may not explain their cytotoxicity.

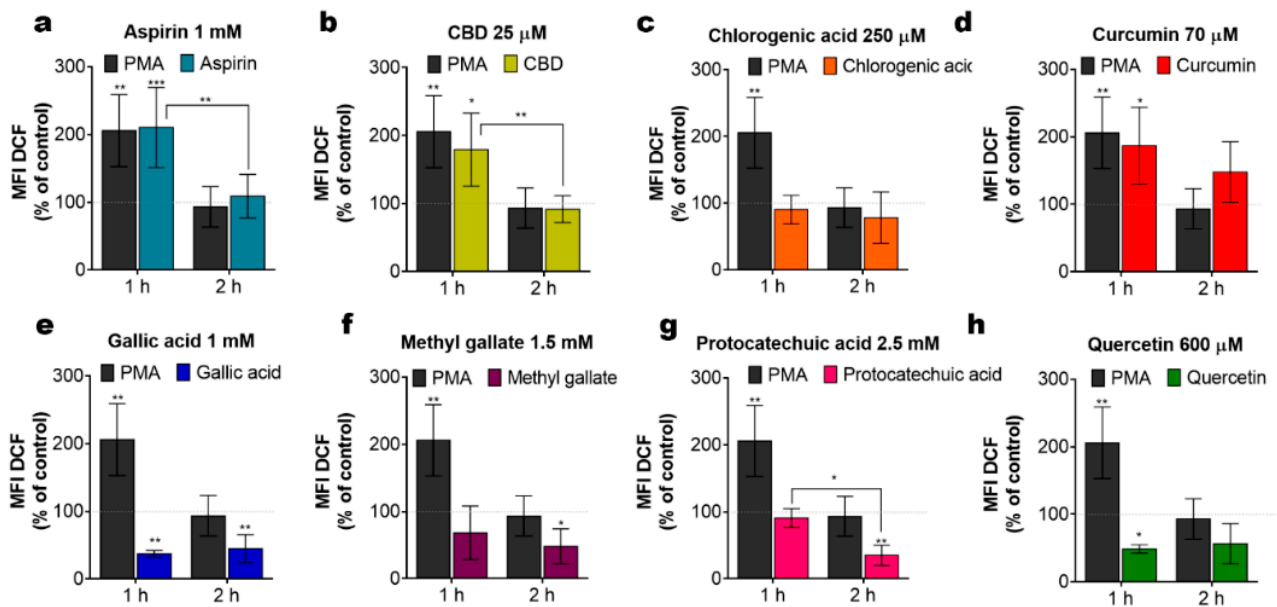


Figure 5. Intrinsic ROS levels in Jurkat cells, treated with different phenolic compounds. (a–h) Cells were stained with the indicator of ROS activity 2', 7'-Dichlorodihydrofluorescein diacetate, DCF-DA (5 μM, 30 min) at 1 h or 2 h of treatment. DCF fluorescence was collected by flow cytometry (10,000 events per sample) and mean fluorescence intensity (MFI) was determined. The MFI value of the untreated cell population was taken as 100% (dotted line). Treatment with phorbol 12 myristate 13 acetate, PMA (5 μM) was used as a positive control. Data are mean ± SD (data from at least three independent experiments; * $p < 0.05$; ** $p < 0.01$; *** $p < 0.001$; two-way ANOVA).

3. Discussion

Our results supported the view that the antileukemic activity of phenolic compounds is due to their interaction with mitochondria in two ways: a direct uncoupling effect (curcumin, quercetin) (Figure 1a,b,e) and mitochondrial Ca^{2+} overload (Figure 3a,b and Figure 4d). Little correlation was found with their pro- or antioxidant activity (Figure 5), albeit the contribution of the former one to the cytotoxicity of CBD and curcumin is not excluded, whereas the antioxidant activity of quercetin may underlie the reversal of cytotoxicity observed at high concentrations of this compound (Figure 1h).

The uncoupling effect of curcumin and quercetin are in line with their predicted protonophore activity [11]. The data in Figure 4e clearly indicate that these compounds suppressed cell metabolic activity and this effect was hardly reverted by Ru360, which inhibits Ca^{2+} uptake mediated by MCU. However, Ru360 prevented CBD- and curcumin-induced cell death (Figure 4d). Thus, mitochondrial Ca^{2+} overload is essential for the execution of the cell death scenario. A large increase in mitochondrial Ca^{2+} , like that induced by CBD, resulted in a stable mPTP formation, collapse of $\Delta\Psi_m$, release of pro-apoptotic factors and, eventually, cell death [10,14]. On the other hand, a moderate increase in $[\text{Ca}^{2+}]_m$ should stimulate oxidative phosphorylation [25], which may be the cause of the $\Delta\Psi_m$ hyperpolarization (Figure 3d) and an increase in the ROS production (Figure 5a), induced by aspirin.

We cannot discard the possibility that bioactive phenols directly activate the MCU, thus promoting the mitochondrial Ca^{2+} overload. On the other hand, those phenolic compounds, which cause a moderate (aspirin) or large (CBD, curcumin) increase in mitochondrial Ca^{2+} were shown to directly interact with VDAC1, favoring its closed conformation [8–10,14], which is preferentially permeable to Ca^{2+} but excludes adenine nucleotides, like ATP [13,26]. We have tested possible protein–ligand interactions between hVDAC1 and different phenols in silico by means of Molegro Virtual Docker. All phenols appear to interact with hVDAC1 within a conserved pocket or cavity, which includes the N-terminal α helix and β 9–13 strands (Figure S1). Of note, the efficient phenols CBD and curcumin

yielded a large number of potentially interacting residues, hence a higher overall binding energy, whereas CBD, curcumin and quercetin had the strongest preference for the two specific residues, His 184 (β 12 strand at the pore wall) and Thr 9 (α helix in the N-terminus) (Figure S1). This may be not just coincidental. Such an interaction may compete with the ligation between certain residues in the N-terminus and a different region in the pore wall, which is thought to fix the VDAC pore fully open [27,28] thus destabilizing the open state vs. the closed one. Alternatively, or additionally, cytotoxic effects of phenols may be due to the detachment of hexokinase from VDAC, which is also induced by hVDAC1 closure or due to the hVDAC1 oligomerization [13,29].

In a conclusion, natural phenols that exhibited the most promising antileukemic effect were CBD and curcumin. These compounds induce the death of T-ALL cells principally via mitochondrial Ca^{2+} overload. Curcumin also exerts an uncoupling effect. Due to its general physicochemical mechanism, the latter will also affect mitochondria in healthy cells. Thus, it remains to be elucidated whether such a dual action would be beneficial or detrimental for T-ALL treatments. As with any small molecules, the aforementioned compounds have multiple cellular targets. For instance, curcumin can positively modulate the extrinsic and intrinsic apoptotic pathways in several types of cancers and enhance the effects of anticancer drugs [30]. Curcumin also inhibits several K^+ channels, including those expressed in lymphocytes and leukemic cells, Kv1.3, Kv11.1 and KCa3.1, and the main lymphocyte Ca^{2+} influx channel CRAC modulates chloride channels, ATP-binding cassette (ABC) and glucose transporters [31]. These effects may be crucial for other cancer types. The efficient inhibition of ABC transporters, including multidrug resistance pumps, by curcumin and by flavonoids (quercetin) [32,33], may have an additional therapeutic effect, by the promotion of the intracellular accumulation of other anticancer drugs. Feasibility and limitations of the clinical potential for each compound must be addressed. For example, the legal status of CBD usage as well the high immunosuppressive effects of curcumin against non-oncological lymphoid cells [34] need to be considered. Another problem is the bioavailability of CBD and curcumin. Published data on their pharmacokinetics revealed a maximal concentration in serum of a few micromoles [35,36]. We see two possible ways to overcome this problem. The first is to develop the chemical derivatives of CBD and curcumin, which will act at lower concentrations. For instance, drugs can be tagged in such a way that make them mitochondria targeted [37]. Another non-exclusive approach is to use the advantage of the drugs' synergism, which can substantially reduce their efficient antileukemic concentration.

4. Materials and Methods

(For technical details please consult Supplementary Table S2).

4.1. Reagents

Reagents used in this study were purchased from Cayman Chemicals (Ann Arbor, Michigan, USA): CBD (90081), chlorogenic acid (70930), gallic acid (11846), methyl gallate (19951), protocatechuic acid (14916), quercetin (10005169); Sigma-Aldrich (San Luis, Missouri, USA): aspirin (A2093), curcumin (C7727), dichlorodihydrofluorescein diacetate (DCFHDA, D6883), phorbol 12 myristate 13 acetate (PMA, P8139); Thermo Fisher Scientific (Waltham, Massachusetts, USA): 4',6-diamidino-2-phenylindole, dihydrochloride (DAPI, D1306), tetramethylrhodamine, ethyl ester, perchlorate (TMRE, T669), Rhod-2 AM, cell permeant (R1244); Merck (Darmstadt, Germany): Ru360 (557440). Phenolic compounds were prepared as stock solutions and maintained at $-20\text{ }^{\circ}\text{C}$ until use: aspirin (134 mM in DMSO), CBD (32 mM in methanol), chlorogenic acid (100 mM in DMSO), curcumin (70 mM in DMSO), gallic acid (150 mM in ethanol), methyl gallate (150 mM in DMSO), protocatechuic acid (250 mM in ethanol), quercetin (150 mM in DMSO). The range of working concentrations used for each drug was in accordance with data available in the literature (Table S1). The highest final solvent concentrations (in *v/v*: 1% DMSO, 0.6% methanol, 0.8% ethanol) did not affect the viability of cells. The effect of phenolic compounds on pH

was verified and no significant changes were observed up to the highest concentration tested.

4.2. Cells and Culture Conditions

Jurkat cell line (clone E6-1, TIB-152) was obtained from the American Type Culture Collection (ATCC, Manassas, VA, USA). Cells between the 3rd and 20th passage counted from the day of receipt were used. Cells were cultured in suspension in a humidified incubator in 5% CO₂ atmosphere at 37 °C. Culture medium was Advanced RPMI 1640 supplemented with 5% (*v/v*) of heat-inactivated fetal bovine serum (FBS), 2 mM GlutaMAX, 10 mM HEPES and 100 U/mL penicillin–100 µg/mL streptomycin (all from Gibco, Thermo Fisher Scientific, Fairport, NY, USA).

4.3. Viability Assay

A resazurin-based metabolic assay in vitro toxicology assay kit Tox8 (Sigma-Aldrich, St. Lois, USA) was used. In this method, non-fluorescent resazurin is reduced to strongly fluorescent resorufin by viable cells. Cells were collected, centrifuged and resuspended in fresh medium (10⁶ cells/mL). The cell suspension (100 µL/well) was placed into a 96-well plate and phenolic compounds were added (in 80 µL/well). After 20 h of incubation, 20 µL of resazurin reagent was added to each well for a total volume of 200 µL. Cells were further incubated for 4 h and the viability was evaluated by measurement of resorufin fluorescence using a GloMax (Promega, Madison, WI, USA) plate reader (Ex: 525 nm, Em: 580–640 nm). Results from independent experiments were averaged and normalized to controls.

4.4. Curcumin Uptake Monitoring

Curcumin is a natural yellow-orange dye, derived from *Curcuma longa*, with previously characterized fluorescent properties [18]. Curcumin fluorescence was measured spectrofluorometrically in a quartz cuvette containing 25 µM of curcumin in PBS. Samples were excited at 405 nm and the emission wavelength was scanned (405–600 nm) to determine the lambda maximum. The fluorescence from 3 independent samples was averaged and plotted. To monitor curcumin uptake, Jurkat cells (1 × 10⁶/mL) were exposed to curcumin (1–100 µM) for 10 min. Upon incubation, cells were washed twice with PBS to remove excess dye, transferred to a 96-well plate and fluorescence was estimated by exciting the samples at 405 nm and collecting the emission fluorescence from 500–550 nm in a GloMax Discover (Promega, Madison, WI, USA) plate reader. To determine subcellular curcumin localization, Jurkat cells were pre-stained with 200 nM of Mitotracker Red (MtRed) for 25 min, washed, suspended in PBS and placed in a custom-made coverslip bottom chambers and evaluated by confocal microscopy (LSM 700, ZEISS microscope). Time-series mode with frame acquisition each minute was used. A single cell was selected and focused and basal fluorescence was acquired prior to curcumin addition (5 frames). Next, curcumin (25 µM) was added and images were acquired for the next 10 min. Raw images were further analyzed in ZEN (ZEISS, Munich, Germany) software to split channels and estimate the fluorescence distribution.

4.5. Mitochondrial Calcium [Ca²⁺]_m Measurements

Jurkat cells were harvested, washed to remove the culture medium and re-suspended in Hanks' balanced salt solution (HBSS; NaCl 143 mM, KCl 6 mM, MgSO₄ 5 mM, CaCl₂ 1.5 mM, HEPES 20 mM, BSA 0.1%, glucose 5 mM, pH 7.4, ≈300 mOsm) for further incubation with the Ca²⁺-sensitive probe Rhod-2AM (2 µM; 30 min; Waltham, MA, USA). Rhod-2 is a cationic dye that preferentially localizes in undamaged mitochondria. After the incubation period, cells were washed to remove extracellular excessive dye, re-suspended in HBSS and assayed 15 min later. Stained cells (1 × 10⁶/mL) were placed in a quartz cuvette. Samples were excited at 552 nm and the Rhod-2 fluorescence was measured at 581 nm using a spectrofluorometer (Hitachi High-Technologies F7000, Hitachinaka, Japan).

Changes in $[Ca^{2+}]_m$ were evaluated as Rhod-2 fluorescence related to initial fluorescence (F/F_0).

4.6. Evaluation of Mitochondrial Membrane Potential ($\Delta\Psi_m$)

Jurkat cells were collected, culture medium was removed, and cells were resuspended in HBSS. Tetramethylrhodamine ethyl ester perchlorate (TMRE, Ex/Em max = 555/582 nm; Thermo Fisher, Waltham, Massachusetts, USA, T669) is a cationic dye that is sequestered and retained by energized mitochondria. Jurkat cells stained with TMRE (200 nM) were exposed to phenolic compounds for 4 or 8 h and changes in TMRE retention was estimated by measurement of fluorescence intensity in a GloMax Discover (Promega, Madison, WI, USA) plate reader. Samples were excited at 549 nm and emission was collected at 575 nm. HBSS or phenols autofluorescence was subtracted and data from independent experiments were averaged and expressed as % to control group.

4.7. Cell Death Analysis by DAPI Retention

Jurkat cells (1×10^6 /mL) were preincubated with Ru360 (1 μ M) for 20 min in RPMI medium in a 48-well plate. After incubation, cells were treated with the selected phenols for 1 h. Right after, cells were collected, washed and resuspended in PBS, then DAPI was added (1 μ M) and incubated for 30 min. Then, cells were washed with PBS to remove excessive dye and DAPI retention was evaluated in a 96-well plate using a GloMax Discover plate reader (Promega, Madison WI, USA) by exciting the samples at 365 nm, while emission was collected at 415–445 nm. Curcumin and quercetin autofluorescence was measured and subtracted to treated cells. Data from independent experiments were averaged and normalized to control group.

4.8. Measurement of ROS by Flow Cytometry

To evaluate the increase or decrease in ROS production caused by the treatment of Jurkat cells with phenolic compounds, the non-fluorescent dye 2', 7'-Dichlorodihydrofluorescein diacetate (DCFH-DA; D6883 Sigma, St. Lois, MO, USA) was used. DCFH-DA is changed to DCF, which is highly fluorescent, when oxidized by intracellular ROS. Jurkat cells were seeded in RPMI cultured medium and treated at indicated concentrations of phenolic compounds by 1–2 h, harvested, washed with PBS and stained with DCFH-DA (100 μ L DCFH-DA 5 μ M/ 5×10^5 cells) for 30 min at 37 °C. DCF fluorescence (Ex/Em: 495 nm/529 nm) was measured by flow cytometry (FACS Canto II, BD Biosciences, Franklin Lakes, NJ, USA) to evaluate changes in intracellular ROS. In these experiments, a 488 laser and a combination of a 502LP mirror and 530/30 filter were used. Debris and doublets were gated out. Ten thousand events (single-cell gate) were collected for each sample. Data analysis was performed with FlowJo 10.2 Software (BD, Ashland, OR, USA) and median intensity fluorescence (MFI) normalized to control was graphed. Cell and phenol autofluorescence was subtracted from DCF-treated and labeled cells.

4.9. Protein–Ligand Interaction Prediction

Molegro Virtual Docker 6.0 software (Odder, Denmark) was used to explore the possible interaction between the phenolic compounds and the human VDAC1 channel. The Pubchem database (NIH) was used to obtain the chemical structure of every phenol studied: aspirin (2244), CBD (644019), chlorogenic acid (1794427), curcumin (969516), gallic acid (370), methyl gallate (7428), protocatechuic acid (72), quercetin (5280343). The hVDAC1 channel structure was downloaded from the protein data bank (PDB, 2JK4). Cavities or possible sites for interaction were detected in the channel structure. MolDock Optimizer was the utilized algorithm and docking was evaluated 20 times for each ligand, considering 1000 possible binding conformations. The best pose was selected for each phenol, based on their docking energy score (MolDock Score). Further analysis for the residues interacting with each molecule was done (ligand map > ligand energy inspector). The amino acid

contribution to the hVDAC1–phenol interaction was depicted by creating a backbone visualization in the workspace.

4.10. Statistical Analysis

Prism 6 (GraphPad Prism software, La Jolla, CA) was employed to perform the analysis. Data are presented as the mean \pm SD. One-way ANOVA and Tukey's multiple comparison test were employed, unless otherwise noted. *p*-values are represented as * ($p \leq 0.05$), ** ($p \leq 0.01$), *** ($p < 0.001$) and **** ($p \leq 0.0001$).

Supplementary Materials: The following are available online at <https://www.mdpi.com/1422-0067/22/1/204/s1>. Table S1, Characteristics of phenolic compounds exhibiting antileukemic activity. Table S2, List of chemicals, cell lines, software, and digitalized molecular structures.

Author Contributions: Conceptualization: M.O.-A., I.P., O.D.; methodology: M.O.-A., L.T.-L.; software: M.O.-A.; validation M.O.-A., L.T.-L., I.P., O.D.; formal analysis: M.O.-A., L.T.-L.; investigation: M.O.-A., L.T.-L.; resources: I.P., O.D.; data curation: M.O.-A., L.T.-L., I.P., O.D.; writing—original draft preparation: M.O.-A.; writing—review and editing: M.O.-A., L.T.-L., I.P., O.D.; visualization: M.O.-A., L.T.-L.; supervision: I.P., O.D.; project administration: I.P., O.D.; funding acquisition: I.P., O.D.; All authors have read and agreed to the published version of the manuscript.

Funding: This work was supported by Consejo Nacional de Ciencia y Tecnología (CONACyT) grants: Ciencia de Frontera 21887 to I.P. and FORDECYT 303072 to O.D. and doctoral fellowships to M.O.-A., and L.T.-L.

Institutional Review Board Statement: Not applicable.

Informed Consent Statement: Not applicable.

Data Availability Statement: The data presented in this study are available in the article and supplementary materials.

Acknowledgments: The authors thank Francisco Olivas-Aguirre from Sonora University (UNISON), who kindly provided some phenolic compounds. The authors also thank Zeferino Gómez for his assistance in docking simulations and Liliana Liñan-Rico for qualified technical assistance.

Conflicts of Interest: The authors declare that they have no known competing financial interests or personal relationships that could have appeared to influence the work reported in this paper.

Abbreviations

ALL	Acute Lymphoblastic Leukemia
CBD	Cannabidiol
CsA	Cyclosporin A
m	Mitochondrial Membrane Potential
MCU	Mitochondrial Calcium Uniporter
ROS	Reactive Oxygen Species
T-ALL	T-lineage ALL
VDAC	Voltage-Dependent Anion Channel

References

1. Siegel, D.A.; Henley, S.J.; Li, J.; Pollack, L.A.; Van Dyne, E.A.; White, A. Rates and trends of pediatric acute lymphoblastic leukemia—United States, 2001–2014. *MMWR Morb. Mortal. Wkly. Rep.* **2017**, *66*, 950–954. [[CrossRef](#)] [[PubMed](#)]
2. Stankovic, T.; Marston, E. Molecular mechanisms involved in chemoresistance in paediatric acute lymphoblastic leukaemia. *Srpski Arhiv za Celokupno Lekarstvo* **2008**, *136*, 1887–1892. [[CrossRef](#)] [[PubMed](#)]
3. Huang, W.Y.; Cai, Y.Z.; Zhang, Y. Natural phenolic compounds from medicinal herbs and dietary plants: Potential use for cancer prevention. *Nutr. Cancer* **2010**, *62*, 1–20. [[CrossRef](#)] [[PubMed](#)]
4. Chen, G.; Wang, F.; Trachootham, D.; Huang, P. Preferential killing of cancer cells with mitochondrial dysfunction by natural compounds. *Mitochondrion* **2010**, *10*, 614–625. [[CrossRef](#)]
5. Mahbub, A.A.; Le Maitre, C.L.; Haywood-Small, S.L.; Cross, N.A.; Jordan-Mahy, N. Polyphenols act synergistically with doxorubicin and etoposide in leukemia cells. *Cell Death Discov.* **2015**, *11*, 5403.
6. Wahle, K.W.L.; Brown, I.; Rotondo, D.; Heys, S.D. *Plant Phenolics in the Prevention and Treatment of Cancer in Bio-Farms for Nutraceuticals. Advances in Experimental Medicine and Biology*; Giardi, M.T., Rea, G., Berra, B., Eds.; Springer: Boston, MA, USA, 2010; pp. 36–51.

7. Salimi, A.; Roudkenar, M.H.; Sadeghi, L. Ellagic acid, a polyphenolic compound, selectively induces ROS-mediated apoptosis in cancerous B-lymphocytes of CLL patients by directly targeting mitochondria. *Redox Biol.* **2015**, *6*, 461–471. [[CrossRef](#)]
8. Tewari, D.; Ahmed, T.; Chirasani, V.R.; Singh, P.K.; Maji, S.K.; Senapati, S.; Kanti Bera, A. Modulation of the mitochondrial voltage dependent anion channel (VDAC) by curcumin. *Biochimica et Biophysica Acta* **2015**, *1848*, 151–158. [[CrossRef](#)]
9. Tewari, D.; Majumdar, D.; Vallabhaneni, S.; Bera, A.K. Aspirin induces cell death by directly modulating mitochondrial voltage-dependent anion channel (VDAC). *Sci. Rep.* **2017**, *7*, 45184. [[CrossRef](#)]
10. Olivas-Aguirre, M.; Torres-López, L.; Valle-Reyes, J.S.; Hernandez-Cruz, A.; Pottosin, I.; Dobrovinskaya, O. Cannabidiol directly targets mitochondria and disturbs calcium homeostasis in acute lymphoblastic leukemia. *Cell Death Dis.* **2019**, *10*, 779. [[CrossRef](#)]
11. Stevens, J.F.; Revel, J.S.; Maier, C.S. Mitochondria-centric review of polyphenol bioactivity in cancer models. *Antioxid. Redox Signal.* **2018**, *29*, 1589–1611. [[CrossRef](#)]
12. Ralph, S.J.; Low, P.; Lawen, A.; Neuzil, J. Mitocans: Mitochondrial targeted anti-cancer drugs as improved therapies and related patent documents. *Recent Pat. Anticancer Drug Discov.* **2006**, *1*, 327–346. [[CrossRef](#)]
13. Olivas-Aguirre, M.; Pottosin, I.; Dobrovinskaya, O. Mitochondria as emerging targets for therapies against T cell acute lymphoblastic leukemia. *J. Leukoc. Biol.* **2019**, *105*, 935–946. [[CrossRef](#)]
14. Rimmerman, N.; Ben-Hail, D.; Porat, Z.; Juknat, A.; Kozela, E.; Daniels, M.P.; Connelly, P.S.; Leishman, E.; Bradshaw, H.B.; Shoshan-Barmatz, V.; et al. Direct modulation of the outer mitochondrial membrane channel, voltage-dependent anion channel 1 (VDAC1) by cannabidiol: A novel mechanism for cannabinoid-induced cell death. *Cell Death Dis.* **2013**, *4*, e949. [[CrossRef](#)] [[PubMed](#)]
15. Colombini, M. VDAC structure, selectivity and dynamics. *Biochimica et Biophysica Acta* **2012**, *1818*, 1457–1465. [[CrossRef](#)] [[PubMed](#)]
16. Magri, A.; Reina, S.; De Pinto, V. VDAC1 as pharmacological target in cancer and neurodegeneration: Focus on its role in apoptosis. *Front. Chem.* **2018**, *6*, 108. [[CrossRef](#)] [[PubMed](#)]
17. Shoshan-Barmatz, V.; Shteinfein-Kuzmine, A.; Verma, A. VDAC1 at the intersection of cell metabolism, apoptosis, and diseases. *Biomolecules* **2020**, *10*, 1485. [[CrossRef](#)] [[PubMed](#)]
18. Chignell, C.F.; Bilski, P.; Reszka, K.J.; Motten, A.G.; Sik, R.H.; Dahl, T.A. Spectral and photochemical properties of curcumin. *Photochem. Photobiol.* **1994**, *59*, 295–302. [[CrossRef](#)]
19. Gorlach, S.; Fichna, J.; Lewandowska, U. Polyphenols as mitochondria-targeted anticancer drugs. *Cancer Lett.* **2015**, *366*, 141–149. [[CrossRef](#)]
20. Moustapha, A.; Pérétout, P.A.; Rainey, N.E.; Sureau, F.; Geze, M.; Petit, J.-M.; Dewailly, E.; Slomianny, C.; Petit, P.X. Curcumin induces crosstalk between autophagy and apoptosis mediated by calcium release from endoplasmic reticulum, lysosomal destabilization and mitochondrial events. *Cell Death Discov.* **2015**, *1*, 15017. [[CrossRef](#)]
21. Zhang, L.; Cheng, X.; Xu, S.; Bao, J.; Yu, H. Curcumin induces endoplasmic reticulum stress-associated apoptosis in human papillary thyroid carcinoma BCPAP cells via disruption of intracellular calcium homeostasis. *Medicine* **2018**, *97*, e11095. [[CrossRef](#)]
22. Sanderson, T.H.; Reynolds, C.A.; Kumar, R.; Przyklenk, K.; Huttemann, M. Molecular mechanisms of ischemia–reperfusion injury in brain: Pivotal role of the mitochondrial membrane potential in reactive oxygen species generation. *Mol. Neurobiol.* **2013**, *47*, 9–23. [[CrossRef](#)] [[PubMed](#)]
23. Rasola, A.; Paolo, B. The mitochondrial permeability transition pore and its adaptive responses in tumor cells. *Cell Calcium* **2014**, *56*, 437–445. [[CrossRef](#)] [[PubMed](#)]
24. Zorov, D.B.; Juhashzova, M.; Sollott, S.J. Mitochondrial reactive oxygen species (ROS) and ROS-induced ROS-release. *Physiol. Rev.* **2014**, *94*, 909–950. [[CrossRef](#)] [[PubMed](#)]
25. Denton, R.M. Regulation of mitochondrial dehydrogenases by calcium ions. *Biochimica et Biophysica Acta* **2009**, *1787*, 1309–1316. [[CrossRef](#)]
26. Tan, W.; Colombini, M. VDAC closure increases calcium ion flux. *Biochimica et Biophysica Acta* **2007**, *1768*, 2510–2515. [[CrossRef](#)]
27. Böhm, R.; Amodeo, G.F.; Murlidaran, S.; Chavali, S.; Wagner, G.; Winterhalter, M.; Brannigan, G.; Hiller, S. The Structural Basis for Low Conductance in the Membrane Protein VDAC upon β -NADH Binding and Voltage Gating. *Structure* **2020**, *28*, 206–214. [[CrossRef](#)]
28. Mertins, B.; Psakis, G.; Grosse, W.; Back, K.C.; Salisowski, A.; Reiss, P.; Koert, U.; Essen, L.-O. Flexibility of the N-Terminal mVDAC1 segment controls the channels gating behavior. *PLoS ONE* **2012**, *7*, e47938. [[CrossRef](#)]
29. Ben-Hail, D.; Begas-Shvartz, R.; Shalev, M.; Shteinfein-Kuzmine, A.; Gruzman, A.; Reina, S.; De Pinto, V.; Shoshan-Barmatz, V. Novel compounds targeting the mitochondrial protein VDAC1 inhibit apoptosis and protect against mitochondrial dysfunction. *J. Biol. Chem.* **2016**, *291*, 24986–25003. [[CrossRef](#)]
30. Reuter, S.; Eifes, S.; Dicato, M.; Aggarwal, B.B.; Diederich, M. Modulation of antiapoptotic and survival pathways by curcumin as a strategy to induce apoptosis in cancer cells. *Biochem. Pharmacol.* **2008**, *76*, 1340–1351. [[CrossRef](#)]
31. Zhang, X.; Chen, Q.; Wang, Y.; Peng, W.; Cai, H. Effects of curcumin on ion channels and transporters. *Front. Physiol.* **2014**, *5*, 94. [[CrossRef](#)]
32. Shukla, S.; Zaher, H.; Hartz, A.; Ware, J.A.; Ambudkar, S.V. Curcumin inhibits the activity of ABCG2/BCRP1, a multidrug resistance-linked ABC drug transporter in mice. *Pharm. Res.* **2009**, *26*, 480–487. [[CrossRef](#)] [[PubMed](#)]
33. Zhang, S.; Yang, X.; Morris, M.E. Flavonoids are inhibitors of breast cancer resistance protein (ABCG2)-mediated transport. *Mol. Pharmacol.* **2004**, *65*, 1208–1216. [[CrossRef](#)] [[PubMed](#)]

34. Sharma, S.; Chopra, K.; Kulkarni, S.K.; Agrewala, J.N. Resveratrol and curcumin suppress immune response through CD28/CTLA-4 and CD80 co-stimulatory pathway. *Clin. Exp. Immunol.* **2007**, *147*, 155–163. [[CrossRef](#)] [[PubMed](#)]
35. Millar, S.A.; Stone, N.L.; Yates, A.S.; O'Sullivan, S.E. A systematic pharmacokinetics of cannabidiol in humans. *Front. Pharmacol.* **2018**, *9*, 1365. [[CrossRef](#)]
36. Shoba, G.; Joy, D.; Joseph, T.; Majeed, M.; Rajendran, R.; Srinivas, P.S. Influence of piperine on the pharmacokinetics of curcumin in animals and human volunteers. *Planta Medica* **1998**, *64*, 353–356. [[CrossRef](#)]
37. Neuzil, J.; Dong, L.; Rohlena, J.; Truksa, J.; Ralph, S.J. Classification of mitocans, anti-cancer drugs acting on mitochondria. *Mitochondrion* **2013**, *13*, 199–208. [[CrossRef](#)]